Cell. Mol. Life Sci. (2012) 69:3115–3125
DOI 10.1007/s00018-012-0983-8

Cellular and Molecular Life Sciences

RESEARCH ARTICLE

# The p38α MAPK positively regulates osteoblast function and postnatal bone acquisition

**Cyril Thouverey · Joseph Caverzasio**

Received: 19 December 2011 / Revised: 14 March 2012 / Accepted: 26 March 2012 / Published online: 20 April 2012


**Abstract** Bone continuously remodels throughout life by coordinated actions of osteoclasts and osteoblasts. Abnormalities in either osteoclast or osteoblast functions lead to bone disorders. The p38 MAPK pathway has been shown to be essential in controlling osteoblast differentiation and skeletogenesis. Although p38α is the most abundant p38 member in osteoblasts, its specific individual contribution in regulating postnatal osteoblast activity and bone metabolism is unknown. To elucidate the specific role of p38α in regulating osteoblast function and bone homeostasis, we generated mice lacking p38α in differentiated osteoblasts. Osteoblast-specific *p38a* knockout mice were of normal weight and size. Despite non-significant bone alterations until 5 weeks of age, mutant mice demonstrated significant and progressive decrease in bone mineral density from that age. Adult mice deficient in *p38a* in osteoblasts displayed a striking reduction in cancellous bone volume at both axial and appendicular skeletal sites. At 6 months of age, trabecular bone volume was reduced by 62 % in those mice. Mutant mice also exhibited progressive decrease in cortical thickness of long bones. These abnormalities correlated with decreased endocortical and trabecular bone formation rate and reduced expressions of type 1 collagen, alkaline phosphatase, osteopontin and osteocalcin whereas bone resorption and osteoclasts remained unaffected. Finally, osteoblasts lacking p38α showed impaired marker gene expressions and defective mineralization in vitro. These findings indicate that p38α is an essential positive regulator of osteoblast function and postnatal bone formation in vivo.

**Keywords** p38α MAPK · Osteoblast · Bone formation · Postnatal

## Introduction

Bone is a dynamic, highly specialized form of connective tissue composed of a mineralized extracellular matrix and three major cell types, i.e., osteoclasts, osteoblasts and osteocytes, which are essential for its structural, mechanical, and metabolic roles. Bone mass and homeostasis is controlled by continuous remodeling throughout life [1]. This process is the consequence of two principal cellular functions, bone resorption and bone formation, which are conducted by osteoclasts and osteoblasts respectively. Dysregulation of the equilibrium between resorption and formation can lead to a variety of bone diseases [1].

Osteoblasts are cells of mesenchymal origin which rebuild resorbed bone by synthesizing proteins of the bone matrix and by inducing matrix mineralization. Those bone-forming cells are also able to regulate osteoclastogenesis and consecutive bone resorption. In spite of significant progress in understanding the molecular basis of osteoblast differentiation during embryonic development, signaling pathways controlling osteoblast functions in postnatal bone remodeling are less understood. Among them, the p38α mitogen-activated protein kinase (MAPK) pathway is suggested as an important regulator of bone homeostasis.

The authors declare that the experiments comply with the current laws of Switzerland in which they were performed.

**Electronic supplementary material** The online version of this article (doi:10.1007/s00018-012-0983-8) contains supplementary material, which is available to authorized users.

C. Thouverey · J. Caverzasio (✉)
Department of Internal Medicine, Service of Bone Diseases, University Hospital of Geneva, 64 Avenue de la Roseraie, 1205 Geneva, Switzerland
e-mail: joseph.caverzasio@unige.ch

C. Thouverey
e-mail: Cyril.Thouverey@unige.ch

The p38 MAPKs belong to the MAPK superfamily and is composed of four members, i.e., p38α, p38β, p38γ, and p38δ [reviewed in 2, 3]. These p38 MAPKs are encoded by distinct genes and share ~60 % of sequence homology. p38 MAPK activation has been shown to occur in response to various extracellular stimuli such as stresses, inflammatory cytokines and growth factors. Despite similar activation, differences exist among the four members and thus each may have highly specific, individual contributions to biologic events [2, 3]. p38 MAPKs have been shown to be implicated in proliferation, differentiation, apoptosis, senescence and cytokine production. p38 MAPKs are activated by MAPK kinase (MKK) 3 and 6 [2, 3]. Several upstream membrane-proximal kinases (MAP3 K) can activate MKK3 and MKK6 including TAK1, ASK1, MKKK4, and MLKs [2, 3].

Previous in vitro studies using cell lines or primary osteoblasts with selective p38 inhibitors have shown that the p38 MAPK pathway regulates alkaline phosphatase activity and extracellular matrix mineralization in response to different osteogenic signals such as BMP-2 [4, 5], TGF-β [5], epinephrine [6], PTH [7], Wnt proteins [8] and mechanical stimuli [9]. Moreover, several reports have also indicated that the p38 pathway regulates the expression and activation of critical transcription factors implicated in osteoblastogenesis, i.e., Dlx5, Runx2, and Osx [5, 10–12].

More recently, an in vivo investigation has highlighted the physiological role of TGF-β-activated kinase 1 (TAK1) in osteoblastogenesis and bone formation [12]. TAK1 is a MAP3 K acting downstream of BMP and TGF-β receptors. Although TAK1 can activate different signaling cascades, the MKK3/6-p38 pathway has been suggested as the main mediator of TAK1 function in osteoblasts [12]. Interestingly, *p38b* knockout mice have been shown to exhibit a low bone mass phenotype suggesting that loss of p38β is not compensated by p38α and therefore, that p38α and p38β may have different functions in bone formation and development [12]. This hypothesis has been confirmed by in vitro analyses demonstrating that p38α regulates early osteoblast differentiation whereas p38β controls late osteoblast maturation [12]. Another MAP3K, mixed-lineage kinase 3 (MLK3) acting downstream of faciogenital dysplasia protein 1, has also been identified as a regulator of osteoblastogenesis and bone development by modulating ERK and p38 MAPK pathways [13]. In addition, the genetic disruption of the neighbor of *Brca1* gene-encoding Nbr1, a receptor for selective autophagosomal degradation of ubiquitinated target proteins, has been shown to induce an age-dependent increase in bone mass due to continuous osteoblastic p38 MAPK activation and subsequent stimulated bone formation [14].

The p38α MAPK is the most abundant p38 member in bone [12]. Although all these previous reports indicate that the p38 MAPK pathway is essential for osteoblast differentiation, the specific individual contribution of p38α in postnatal bone formation remains to be elucidated. To investigate the role of p38α in regulating postnatal osteoblast function and bone homeostasis in vivo, we therefore generated mice for which the p38α-encoding gene was specifically disrupted in differentiated osteoblasts after birth by using Cre-LoxP technology. The bone phenotypes of control and osteoblast-specific *p38a* knockout mice were analyzed and compared at different ages. Osteoblast-specific excision of *p38a* led to age-dependent decrease in bone mass and bone mineral density. This low bone mass phenotype was observed in axial and appendicular bones. It was the consequence of defective osteoblast function and impaired endocortical and trabecular bone formation. Our results provide the first evidence that the p38α MAPK is a critical regulator of postnatal osteoblastic bone formation.

## Materials and methods

### Generation of conditional *p38a* knockout mice

Mice lacking p38α in osteoblasts were generated by breeding mice harboring floxed p38α-encoding gene (*p38a* with LoxP sites flanking exons 2 and 3; Fig. 1a) [15] with mice expressing the Cre recombinase under the control of the osteocalcin promoter (*Ocn-Cre*) [16]. *Ocn-Cre* mice, in which Cre expression exclusively occurs in osteoblasts at birth [16], represent a unique tool to address postnatal osteoblast function. Mice homozygous for floxed *p38a* alleles ($p38a^{f/f}$) were crossed with *Ocn-Cre* mice to generate *Ocn-Cre*;$p38a^{f/+}$ mice. These mice were then crossed with $p38a^{f/f}$ mice to generate *Ocn-Cre*;$p38a^{f/f}$ mice (Δ*p38a*). Cre-mediated excision of exons 2 and 3, which encode the ATP-binding site of the p38α kinase domain, has been shown to result in *p38a*-null alleles [15, 17]. Δ*p38a* mice were healthy and fertile and used for subsequent crosses. Mice were maintained under standard non-barrier conditions, and had access to mouse diet RM3 containing 1.24 % calcium and 0.56 % available phosphorus (SDS, Betchworth, UK) and water ad libitum. Genotyping of the wild-type, floxed, and excised p38α-encoding gene were carried out by PCR. All performed experiments were in compliance with the *Ethical Principles and Guidelines for Scientific Experiments on Animals* (2nd edition) and approved by the Ethical Committee of the University of Geneva School of Medicine and the State of Geneva Veterinarian Office.

### Dual-energy X-ray absorptiometry and μ-CT

Mice were anesthetized through intraperitoneal injection of ketamine/xylazine and placed on a tray in a mouse

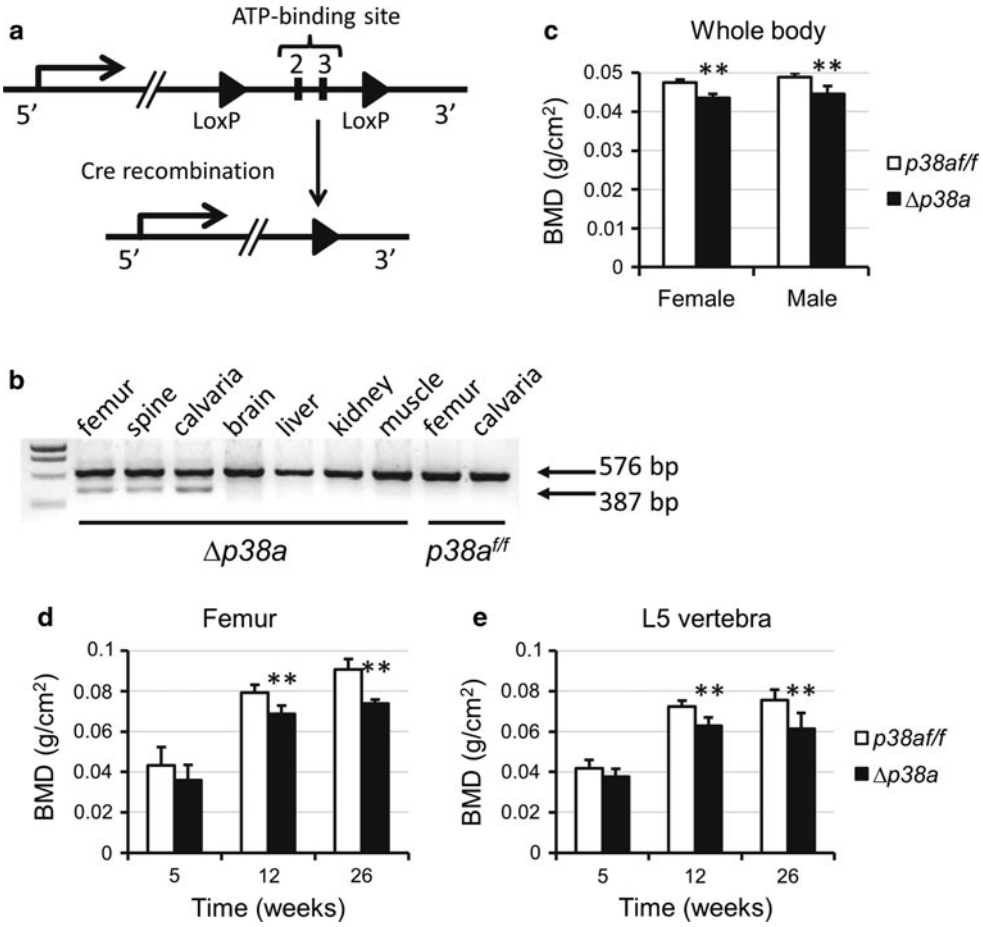


**Fig. 1** Disruption of *p38a* in osteoblasts leads to decreased BMD. **a** Strategy for the generation of mice with LoxP-flanked *p38a* alleles [15]. Exons 2 and 3 which encode the ATP-binding site of the kinase domain were flanked by two LoxP sequences (shown as *black arrowheads*). Cre-mediated deletion produces the Δ*p38a* allele. **b** RT-PCR detection of *p38a* (576 bp) and of Δ*p38a* lacking exons 2/3 (387 bp) in tissues from $p38a^{flox/flox}$ ($p38a^{f/f}$) and *Ocn-Cre*;$p38a^{flox/flox}$ mice (Δ*p38a*). Osteocalcin promoter-driven deletion of exons 2 and 3 was only detected in skeletal tissues of Δ*p38a* mice. **c** Whole body BMD of female and male $p38a^{f/f}$ and Δ*p38a* mice at 12 weeks of age ($n = 6$ per group). **d** Femoral and **e** lumbar BMD of female $p38a^{f/f}$ and Δ*p38a* mice at 5, 12 and 26 weeks of age. $^{**}p \leq 0.01$

densitometer (PIXImus II, GE Lunar, Madison, WI) for analysis. Total body, femoral and spinal bone mineral densities (BMD) were measured in vivo. Mice were then sacrificed by cervical dislocation and their bones were excised for micro-computed tomography (μCT) analyses. Trabecular bone microarchitecture of 5th lumbar vertebral bodies and distal femurs, and cortical bone geometry of femoral midshafts were assessed using μCT (micro-CT40, Scanco Medical AG, Basserdorf, Switzerland). Femurs and vertebrae were scanned with an isotropic voxel size of 12 μm.

## Histological and histomorphometric analysis

To measure dynamic indices of bone formation, 12-week-old mice received subcutaneous injections of calcein (10 mg/kg body weight; Sigma) at 9 and 2 days before euthanasia and bone collection. After dehydration in a graded ethanol solution series, undecalcified femurs were embedded in methyl methacrylate (Merck), and 8-μm transversal sections of midshafts were cut using a MET-KON Finocut low-speed precision cutter and mounted unstained for fluorescence evaluation. 5-μm sagittal sections of distal femurs were cut with a Polycut E microtome (Leica Corp. Microsystems AG, Glattbrugg, Switzerland) and mounted unstained for fluorescence visualization or stained with modified Goldner's trichrome. Histomorphometric measurements were carried out on the endocortical and periosteal surfaces of femoral midshaft sections and on the secondary spongiosa of distal femur sections using a Leica Q image analyzer at 40× magnification as previously described [18].

## ELISA assays

Sera were collected from 12-week-old mice and tartrate-resistant acid phosphatase 5b (TRAP5b, a marker of bone resorption) levels determined by ELISA according to the manufacturer's instructions (Immunodiagnostic Systems Ltd).

## Primary osteoblast cultures

Primary osteoblasts were isolated from long bone metaphyses of 12-week-old control and osteoblast-specific *p38a* knockout mice as recently described [19]. Mice were sacrificed by cervical dislocation and rinsed in 70 % ethanol for 5 min. Humeri, tibiae and femurs were dissected

and their epiphyses removed. Bone marrow was flushed out and bone cavities were washed several times with α-MEM (Amimed, Bioconcept) supplemented with 10 % FBS, 1 % penicillin/streptomycin and 2.2 g/L L-glutamine (all from Gibco). Bones were then cut into small chips and incubated in α-MEM containing 10 % FBS and 1 mg/mL collagenase II (Sigma) for 90 min on a shaking incubator at 37 °C. Digestion medium and released cells were discarded. Bone chips were washed several times with medium and incubated in α-MEM containing 10 % FBS at 37 °C in a 5 % $CO_2$/95 % air humidified atmosphere for 3 days to allow osteoblast migration from bone fragments. After 5 days, cell cultures were trypsinized (with trypsin/EDTA from Sigma) and passaged at a split ratio of 1:3. Bone fragments and osteoblasts were seeded together for at least 3 additional days. At the second passage, bone chips were removed. The medium was changed every 2–3 days. Osteoblasts at passages 3–4 were used for in vitro experiments.

### Proliferation and differentiation assays

To assess osteoblast proliferation, cells were seeded at 40,000 cells/well in 12-well plates with α-MEM containing 10 % FBS and counted after 6 days using a cell counter (Coulter Counter). For differentiation assays, osteoblasts that reached confluence were incubated in osteogenic medium containing α-MEM, 10 % FBS, 0.05 mM L-ascorbate-2-phosphate (Sigma) and 10 mM β-glycerophosphate (AppliChem GmbH). After 10 days, alkaline phosphatase activity was measured as previously described [6–8]. After 21 days, matrix mineralization was evaluated by Alizarin Red-S staining (AR-S; Sigma). To quantify mineral-bound AR-S, cell cultures were destained with 10 % hexadecylpyridinium chloride (Sigma) and AR-S concentration was determined by measuring the absorbance at 562 nm. In these experiments, the effect of SD-282, a selective p38α inhibitor (SCIOS, Fremont, CA), were also tested.

### RNA isolation, RT-PCR and real-time PCR

Total RNA was extracted from murine femurs or primary osteoblasts using peqGOLD TriFast™ (peqlab Biotechnologie GmbH) and purified using an RNeasy Mini Kit (Qiagen) [18]. Single-stranded cDNA was synthesized from 2 µg of total RNA using a High-Capacity cDNA Archive Kit (Applied Biosystems) according to the manufacturer's instructions. RT-PCR, with primers surrounding *p38a* exons 2 and 3, was used to check Cre-mediated excision of those two exons in bones of Δ*p38a* mice (Fig. 1b). Real-time PCR was performed to measure the relative mRNA levels using the StepOnePlus™ Real-Time PCR System with SYBR Green (Applied Biosystems). The primers used in our analyses are indicated in the supplementary materials (Table S1). The mean mRNA levels were calculated from triplicate analyses of each sample. Obtained mRNA level for a gene of interest was normalized to β2-microglobulin mRNA level in the same sample.

### Statistical analysis

All results were expressed as mean ± standard deviation. All statistical analyses were performed using the Student's *t* test. Differences were considered as significant when $p < 0.05$.

## Results

### Generation of mice lacking p38α in osteoblasts

To investigate the role of p38α in regulating postnatal osteoblast function and bone homeostasis in vivo, we generated mice lacking p38α in their differentiated osteoblasts. *Ocn-Cre;p38a*$^{f/f}$ mice, which were viable and fertile, were crossed with *p38a*$^{f/f}$ mice to obtain control (*p38a*$^{f/f}$) and *Ocn-Cre;p38a*$^{f/f}$ (referred to as Δ*p38a*) littermates with expected Mendelian ratio. Excision of *p38a* exons 2 and 3 was checked in different tissues by RT-PCR using primers surrounding those two exons. A band corresponding to wild-type *p38a* (576 bp) was observed in all tissues whereas a band corresponding to *p38a* lacking exons 2/3 (387 bp) was only detected in femurs, calvaria and spines of Δ*p38a* mice showing that Cre-mediated deletion only occurred in skeletal tissues of Δ*p38a* mice (Fig. 1b).

### Low BMD in adult mice lacking p38α in osteoblasts

A longitudinal analysis of bone mineral density was performed by using dual-energy X-ray absorptiometry. Mice carrying an osteoblast-specific deletion of *p38a* had normal body weight and size throughout life (data not shown). At 12 weeks of age, Δ*p38a* mice of both sexes displayed significant decrease in whole body BMD in comparison to their control littermates ($p < 0.01$; Fig. 1c). BMD was similarly decreased in both axial and appendicular skeletal sites at 12 weeks of age ($p < 0.001$; Fig. 1d, e). There was only a non-significant trend at 5 weeks but, then femoral and lumbar BMD progressively decreased as the animals aged (Fig. 1d, e). Both femoral and lumbar BMD of 26-week-old female Δ*p38a* mice were significantly decreased by 19 %.

### Low cortical and trabecular bone mass in adult Δ*p38a* mice

Bone microarchitecture of $p38a^{f/f}$ and Δ*p38a* mice was evaluated by three-dimensional μCT scanning analyses. Femoral length and diameter of Δ*p38a* mice were normal in comparison to those of $p38a^{f/f}$ mice. However, Δ*p38a* mice of both sexes displayed significant alterations of femoral microarchitecture at 12 weeks of age (supplementary Table S2). Consistent with BMD data, a longitudinal analysis performed on female mice revealed non-significant decreases in cortical and trabecular bone volumes at 5 weeks and then progressive reductions as the animals aged ($p \leq 0.002$; Figs. 2c, 3b). At the femoral midshaft, the total volume and cross-sectional area remained unchanged between mutant and control mice (Fig. 2a, b). However, Δ*p38a* adult mice showed decreased cortical thickness (−20 %, $p \leq 0.0003$; Fig. 2d). In addition, adult mutant mice also displayed significant reduction in trabecular bone volume ($p \leq 0.002$; Fig. 3b) associated with low trabecular thickness ($p \leq 0.05$; Fig. 3c) at the distal femur. Decreased trabecular number and increased trabecular separations became significant at the distal femurs of 26-week-old mutant mice ($p = 0.01$; Fig. 3d, e). At that age, femoral trabecular bone volume was reduced by 62 % in Δ*p38a* mice ($p = 0.0007$; Fig. 3b). A similar pattern of low trabecular bone mass was observed at the 5th lumbar vertebral body of 12-week-old Δ*p38a* mice (supplementary Fig. S1).

### Low bone formation and unaffected bone resorption in adult Δ*p38a* mice

Histomorphometric analyses by double calcein labeling were carried out on femurs of $p38a^{f/f}$ and Δ*p38a* mice at 12 weeks of age to measure dynamic indices of bone formation. Mutant mice displayed reduced endocortical and trabecular mineral apposition rate (MAR), mineralizing surfaces (MS/BS) and bone formation rate (BFR) (Table 1). Those reductions were more pronounced in trabecular bone sites (Table 1). Furthermore, periosteal MAR was slightly decreased in Δ*p38a* mice but MS/BS and BFR were not significantly reduced at periosteal bone surfaces (Table 1). Even though mutant mice showed striking reduction of bone formation in trabecular bone (Fig. 4a, b), static histomorphometric analyses did not reveal significant changes in number of osteoblasts lining trabecular bone surfaces (Fig. 4c, d). However, functional defects of osteoblasts could be explained by significant lower expressions of type 1 collagen (*Col1a1*; −45 %; $p = 0.05$), alkaline phosphatase (*Alp*; −50 %; $p = 0.02$), osteopontin (*Opn*; −64 %; $p = 0.05$) and osteocalcin (*Ocn*; −56 %; $p = 0.005$) (Fig. 4e) in the long bone of Δ*p38a* mice. Nevertheless, expression of the master regulator of osteoblast development, i.e., Runx2, remained unchanged between control and mutant mice (Fig. 4e). These data demonstrated an impaired bone formation by osteoblasts lacking p38α.

Furthermore, ex vivo gene expression analyses also revealed a reduction of both rank ligand (*Rankl*) and

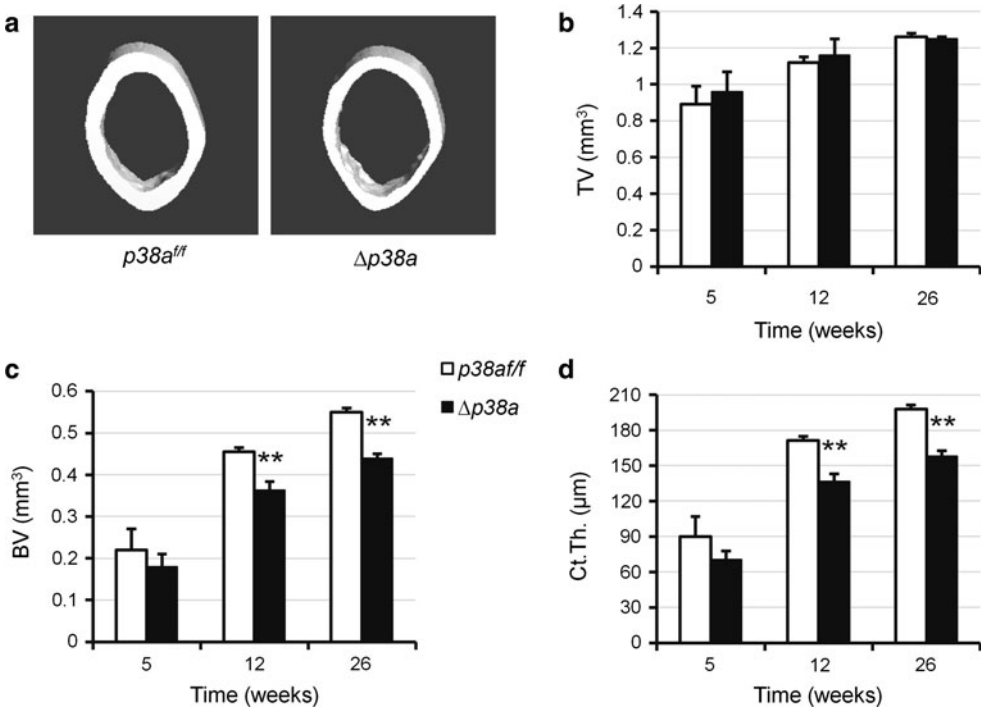


**Fig. 2** Mice lacking p38α in their osteoblasts exhibit low cortical bone mass. **a** Representative reconstructed μCT images of femoral midshafts from 12-week-old female $p38a^{f/f}$ versus Δ*p38a* mice. **b–d** Cortical bone microarchitecture was measured at femoral midshaft of female $p38a^{f/f}$ and Δ*p38a* mice at 5 ($n = 4$ per genotype), 12 ($n = 6$ per genotype) and 26 ($n = 4$ per genotype) weeks of age. μCT parameters include **b** *TV* total volume, **c** *BV* bone volume and **d** *Ct.Th.* cortical thickness. $^{**}p \leq 0.01$

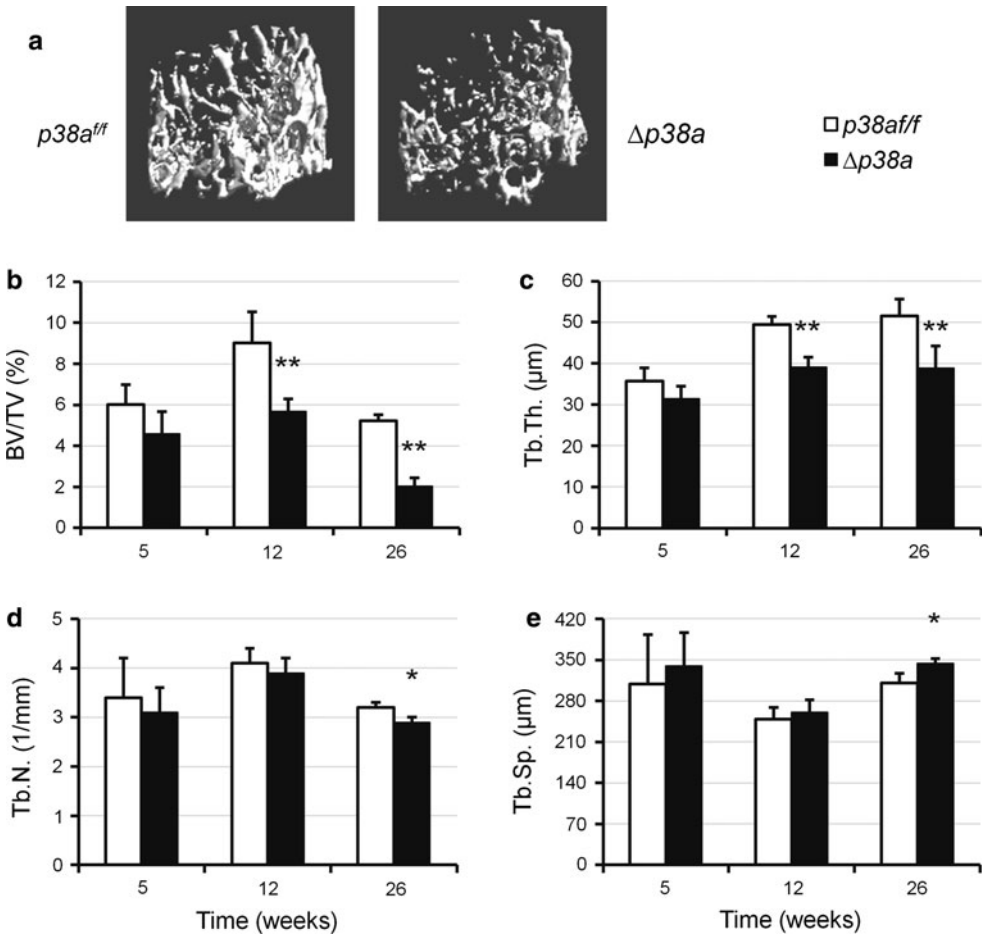


**Fig. 3** Mice lacking p38α in their osteoblasts have low trabecular bone mass. **a** Representative reconstructed μCT images of distal femurs from 12-week-old female *p38a*$^{f/f}$ versus Δ*p38a* mice. **b–e** Trabecular bone microarchitecture was measured at distal femur of female *p38a*$^{f/f}$ and Δ*p38a* mice at 5 ($n = 4$ per genotype), 12 ($n = 6$ per genotype) and 26 ($n = 4$ per genotype) weeks of age. μCT parameters include **b** *BV/TV* bone volume/total volume, **c** *Tb.Th.* trabecular thickness, **d** *Tb.N.* trabecular number, **e** *Tb.Sp.* trabecular separation. $^{*}p < 0.05$, $^{**}p \leq 0.01$

**Table 1** Bone formation indices from 12-week-old *p38a*$^{f/f}$ and Δ*p38a* female mice

| | Parameters | *p38a*$^{f/f}$ | Δ*p38a* | *p* values | Δ (%) |
|---|---|---|---|---|---|
| Periosteal | Ps-MAR (μm/d) | 1.23 ± 0.10 | 1.06 ± 0.10 | 0.009 | −13.80 |
| | Ps-MPm/BPm (%) | 42.1 ± 16.6 | 39.3 ± 9.3 | 0.71 | – |
| | Ps-BFR/BPm (μm/d) | 0.52 ± 0.21 | 0.42 ± 0.12 | 0.30 | – |
| Endocortical | Ec-MAR (μm/d) | 1.21 ± 0.13 | 0.93 ± 0.15 | 0.007 | −23.10 |
| | Ec-MPm/BPm (%) | 42.2 ± 5.7 | 31.1 ± 5.6 | 0.005 | −26.30 |
| | Ec-BFR/BPm (μm/d) | 0.51 ± 0.07 | 0.29 ± 0.07 | 0.0002 | −43.10 |
| Trabecular | Tb-MAR (μm/d) | 1.03 ± 0.07 | 0.76 ± 0.10 | 0.001 | −26.20 |
| | Tb-MS/BS (%) | 53.8 ± 11.0 | 34.6 ± 13.4 | 0.03 | −35.70 |
| | Tb-BFR/BS (μm/d) | 0.55 ± 0.12 | 0.26 ± 0.10 | 0.002 | −52.70 |

Dynamic histomorphometric analyses were performed at femoral diaphyses (periosteal and endocortical) and distal femurs (trabecular) of control (*p38a*$^{f/f}$) and mutant (Δ*p38a*) female mice ($n = 6$ per group)

Data are expressed as mean ± SD. *p* values were determined using unpaired *t* tests. Significant differences are expressed as percentage

*MAR* mineral apposition rate, *MPm* mineralizing perimeter, *BPm* bone perimeter, *MS* mineralizing surface, *BS* bone surface, *BFR* bone formation rate

osteoprotegerin (*Opg*) expressions (Fig. 5a) in the long bone of Δ*p38a* mice. However, these effects were not significant and the relative *Rankl*/*Opg* ratio was not significantly changed (Fig. 5a). Consistent with this observation, the number of mature osteoclasts covering trabecular bone surfaces and serum TRAP5b levels

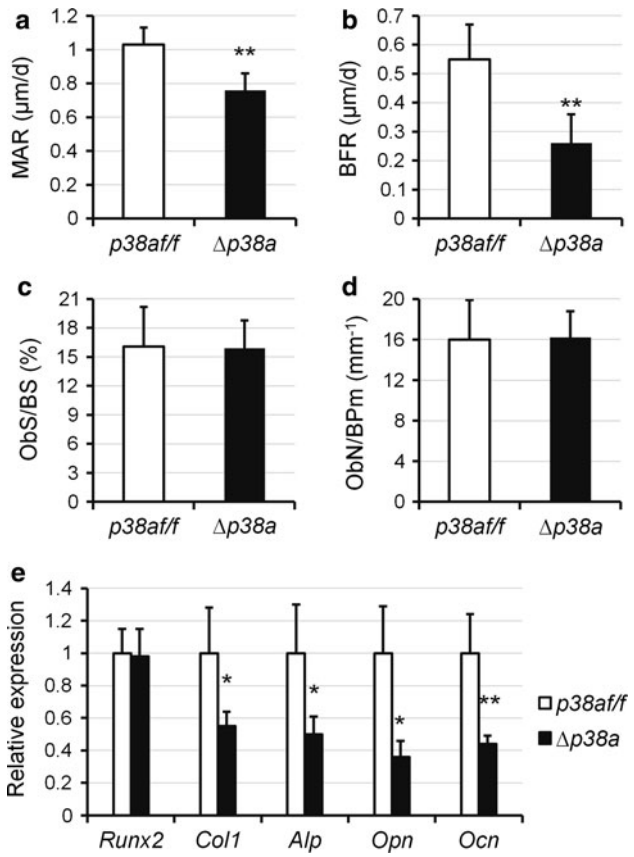


**Fig. 4** Osteoblast-specific disruption of *p38a* decreases bone formation in mice. **a**–**d** Quantitative histomorphometric measurements were performed on the spongiosa at distal femurs of 12-week-old female $p38a^{f/f}$ and Δ*p38a* mice ($n = 6$ per group). **a** *MAR* mineral apposition rate; **b** *BFR* bone formation rate; **c** *ObS/BS* osteoblast surface/bone surface; **d** *ObN/BPm* osteoblast number/bone perimeter. **e** Real-time PCR analyses of osteoblast marker gene expression in femurs of 12-week-old female $p38a^{f/f}$ and Δ*p38a* mice ($n = 6$ per group). $^{*}p < 0.05$, $^{**}p \leq 0.01$

remained unchanged between control and mutant mice (Fig. 5b–d). These results indicated that loss of p38α did not affect osteoclasts and bone resorption.

### Suppressed marker expressions and mineralization in osteoblasts lacking p38α

To further explore the cellular mechanism explaining the low bone mass of osteoblast-specific *p38a* knockout mice, the phenotype of *p38a* knockout osteoblasts were analyzed in vitro. In cultures, osteocalcin promoter-driven deletion of *p38a* started 2 or 3 days after Δ*p38a* osteoblasts reached confluence and was maximal after approximately 7 days. At that time-point, expression was reduced by 65 % in cultures of Δ*p38a* osteoblasts compared with those of $p38a^{f/f}$ osteoblasts ($p = 0.0001$; Fig. 6a). Interestingly, *p38a* deletion was not compensated by overexpression of genes encoding p38β, p38γ, and p38δ (supplementary Fig. S2). Cell counting performed after confluence did not reveal changes in number of Δ*p38a* osteoblasts compared with $p38a^{f/f}$ osteoblasts (results not shown). This result was confirmed with the use of SD282, a selective p38α inhibitor, in growing wild-type osteoblast cultures (Fig. 6e), indicating that the p38α MAPK pathway did not affect osteoblast proliferation. Osteoblast phenotype was first evaluated using quantitative real-time PCR. Expression of *Runx2* was not affected by *p38a* deletion whereas mRNA expression levels of *Col1a1*, *Alp*, *Opn* and *Ocn* were significantly decreased in Δ*p38a* osteoblasts (−54, −60, −39 and −50 % respectively; Fig. 6a). Moreover, alkaline phosphatase (ALP) activity was significantly reduced in Δ*p38a* osteoblast cultures ($p = 0.0001$; Fig. 6b). Consistent with this observation, SD282 dose-dependently inhibited basal, TGFβ1- and BMP2-induced ALP activity and mineralization (Fig. 6f; supplementary Fig. S3). Finally, in vitro matrix mineralization was almost suppressed in Δ*p38a* osteoblast cultures, as shown by alizarin red staining ($p = 0.0001$; Fig. 6c, d). Those results clearly showed that p38α is a positive regulator of osteoblast function and that loss of p38α could not be compensated by other p38 members.

## Discussion

Postnatal bone remodeling requires an accurate balance between bone resorption by osteoclasts and bone formation by osteoblasts [1]. Dysregulations of osteoclast and osteoblast activities are associated with a range of pathological diseases such as osteoporosis which is characterized by low bone mass and microarchitectural deterioration of bone tissue, with a consequent increase in bone fragility [20, 21]. Due to the increasing need for anabolic therapies to prevent age-related bone loss, research has been focused over the last decade on molecular mechanisms regulating osteoblast function in postnatal remodeling [20–22]. For instance, Runx2 and Osx have been found to regulate osteoblast function in adult bone in addition to their primarily established role in osteoblastogenesis [23, 24]. Another transcription factor, Atf4 regulates bone matrix deposition by mature osteoblasts [25]. Furthermore, several signaling pathways have been shown to regulate postnatal osteoblast function including Ihh [26], Wnt/Lrp5 [27], TGFβ-BMP/Smads [28–30], BMP/MEKK2/MEK5-7/Jnk [31], β-adrenergic [32], IGF-1 [16], insulin [33] and PTH signaling [34].

The p38 MAPK pathway has been recently shown to be an essential regulator of osteoblastogenesis during skeletogenesis [12, 13]. Indeed, mice lacking MKK3 and MKK6 (upstream activators of p38 MAPK) exhibited low bone mass phenotype at 3 weeks of age, due to impaired

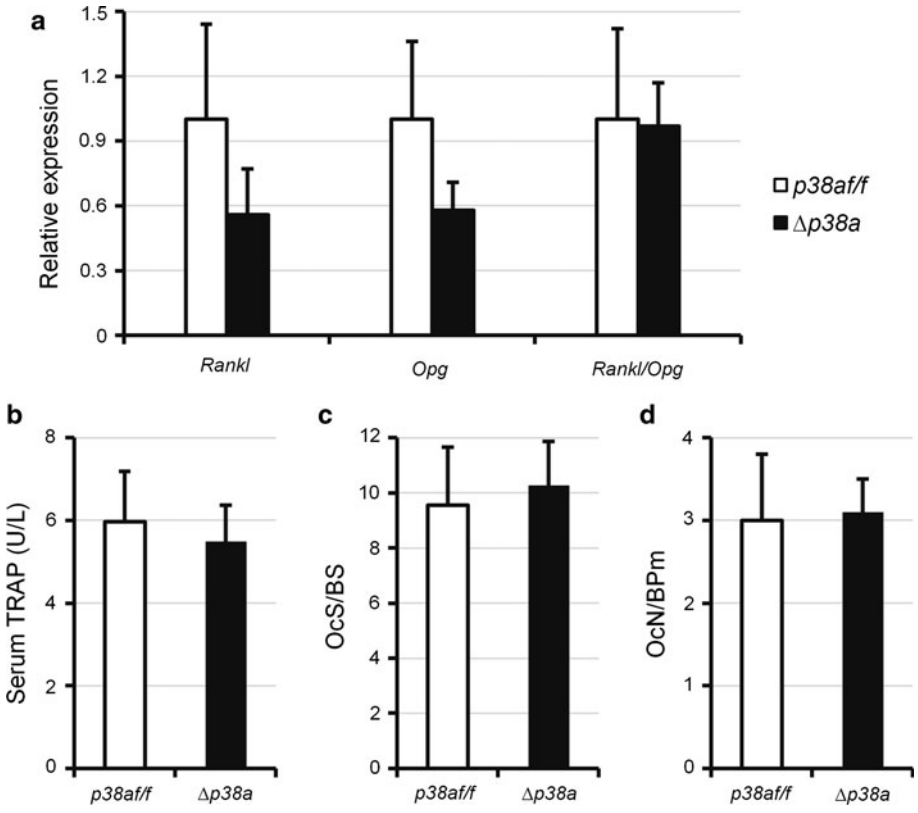


**Fig. 5** Osteoblast-specific disruption of *p38a* does not affect bone resorption. **a** Real-time PCR analyses of *Rankl* and *Opg* expression in femurs of 12-week-old female $p38a^{f/f}$ and Δ*p38a* mice. **b** Detection of TRAP5b in serum of 12-week-old female $p38a^{f/f}$ and Δ*p38a* mice by ELISA. **c**, **d** Quantitative histomorphometric measurements were performed on the spongiosa at distal femurs of 12-week-old female $p38a^{f/f}$ and Δ*p38a* mice. **c** *OcS/BS* osteoclast surface/bone surface; **d** *OcN/BPm* osteoclast number/bone perimeter. $n = 6$ per group in each experiment

osteoblast differentiation and reduced bone formation [12]. Mice lacking p38$\beta$ also displayed low bone mass since *p38b* knockout osteoblasts failed to differentiate into mature osteoblasts [12]. However, the physiological role of the p38 MAPK pathway in regulating postnatal bone formation remained to be investigated.

Since p38α is the most abundant p38 member in bone and osteoblasts [12], the present work aimed to elucidate its individual contribution in regulating postnatal osteoblast function. Therefore, we used mice in which *p38a* was specifically deleted in osteoblasts by postnatal Cre recombination under the control of the osteocalcin promoter. Mice lacking p38α in their differentiated osteoblasts had normal size and weight, and did not show any significant bone abnormalities before 5–6 weeks of age, indicating that p38α MAPK in osteoblasts does not regulate radial bone growth and bone modeling, two active and predominant processes during mouse growth [35]. However mutant mice started to exhibit dramatic and progressive decrease in BMD and bone microarchitectural alterations from that age. These effects were observed in both axial and appendicular skeletons of both sexes (Fig. 1c–e). Cortical thickness that gives strength to long bones was reduced by 20 % in adult mutant mice whereas cross-sectional area remained unaffected (Fig. 2). This observation correlated well with reduced endosteal MAR, MS/BS and BFR while those parameters were not (or slightly) changed at periosteal surfaces (Table 1). The most striking effect observed in adult Δ*p38a* mice was the dramatic and age-dependent reductions in trabecular bone volume and trabecular thickness (Fig. 3). For instance, trabecular bone volume was decreased by 62 % at the distal femur of 26-week-old mutant mice (Fig. 3b). This was associated with an important decrease in trabecular bone formation (Fig. 4a, b). Decreased bone formation was not explained by changes in osteoblast number (Fig. 4c, d) but rather by impaired osteoblast function since *Col1a1*, *Alp*, *Opn* and *Ocn* expressions were reduced in the long bones of mutant mice (Fig. 4e). The osteoblast-specific deletion of *p38a* did not affect osteoclast number and activity in bones (Fig. 5), indicating that p38α is not required for osteoblast-mediated control of osteoclastogenesis and bone resorption, consistent with previous findings [12]. Mice lacking p38α clearly displayed an age-dependent osteoporotic phenotype. This low bone mass phenotype occured when bone remodeling became a predominant process after 6 weeks of age, indicating that osteoblasts were unable to fully replace resorbed bone.

Alteration of osteoblast-mediated bone formation in absence of p38α was further supported by in vitro analyses. In cultures, Cre-mediated deletion of *p38a* occurred when Δ*p38a* osteoblasts stopped proliferating and started to differentiate. In addition, inhibition of p38α MAPK with a selective inhibitor during the proliferation phase of wild-

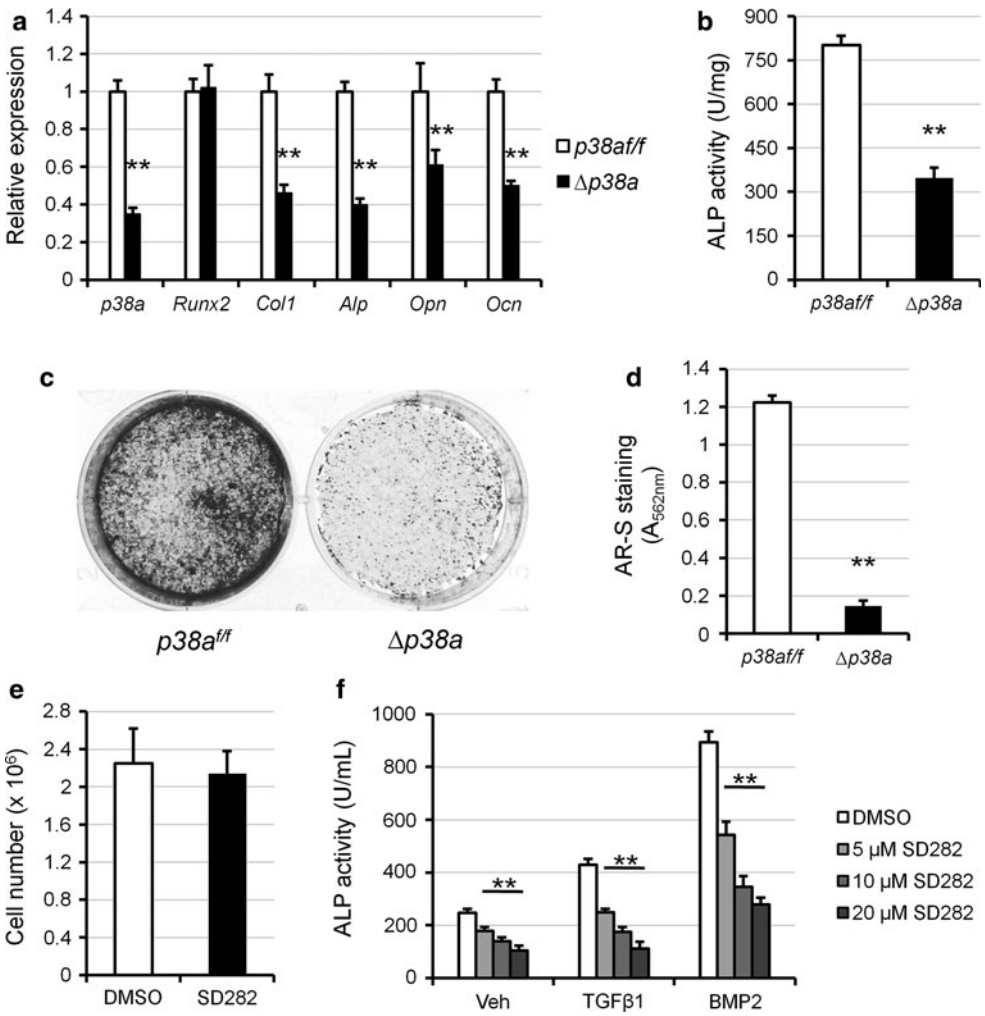


**Fig. 6** Osteoblasts lacking p38α exhibit a defective function in vitro. **a–d** Primary osteoblasts were isolated from the long bones of $p38a^{f/f}$ and Δ*p38a* mice and their phenotypes were compared. **a** Osteoblast marker gene expression was assessed by real-time PCR after 7 days of culture in osteogenic medium. **b** Alp activity was measured after 10 days of culture in osteogenic medium. **c** Representative images and **d** quantification of matrix mineralization evaluated by Alizarin Red-S (AR-S) staining after 21 days of culture. **e**, **f** Primary osteoblasts were isolated from wild type mice and cultured in the absence (vehicle: DMSO) or presence of SD282, a selective p38α inhibitor. **e** Cell number was measured by counting cells cultured for 7 days in the absence or presence of 10 μM SD282. **f** Alp activity was measured in osteoblasts co-treated with different doses of SD282 and vehicle, TGF$\beta$1 (5 ng/mL) or BMP2 (50 ng/mL) for 4 days. $^{**}p \leq 0.01$

type osteoblasts did not influence cell number (Fig. 6e). Those results were consistent with unchanged osteoblast number in Δ*p38a* mutant mice (Fig. 4c, d). Moreover, osteoblasts lacking p38α were less active than control osteoblasts as shown by reduced ALP activity, decreased expressions of *Col1a1*, *Alp*, *Opn* and *Ocn*, and suppressed mineralization in vitro (Fig. 6). It is interesting to note that lack of p38α in osteoblasts exclusively impaired bone formation at sites of intense remodeling (trabecular and endosteal surfaces; Table 1), suggesting that p38α could be a necessary pathway in osteoblasts to couple bone formation to resorption. One proposed coupling mechanism is the local release of factors such as TGF$\beta$1, BMP2, or IGF1 by resorption [1]. This hypothesis was further supported by our experiments in which osteoblasts treated with a selective inhibitor of p38α were unable to respond to osteogenic ligands such as TGF$\beta$1 and BMP2 (Fig. 6f; supplementary Fig. S3b).

The age-dependent decrease in bone mass induced by osteoblast-specific deletion of *p38a* supports previous observations of Whitehouse et al. [14] in their homozygous truncated Nbr1 (trNbr1) mutant mice. Genetic truncation of Nbr1, a receptor for selective autophagosomal degradation of ubiquitinated target proteins, was shown to induce an age-dependent increase in bone mass due to stimulated bone formation. Unlike the full-length protein, trNbr1 could not bind activated p38 MAPK and target it for degradation. In cultures, trNbr1 osteoblasts were highly active and had elevated activation of p38 MAPK. The pharmacological inhibition of p38 MAPK could abrogate the increased trNbr1 osteoblast activity [14]. Interestingly, the bone phenotype of our Δ*p38a* mutant mice was the opposite to that of trNbr1 mutant mice.

In conclusion, this report shows that the osteoblast-specific disruption of *p38a* leads to a progressive decline of postnatal bone mass due to defective osteoblast function. It clearly demonstrates that the p38α MAPK is a critical positive regulator of postnatal osteoblastic bone formation. It has been previously reported that the p38α MAPK pathway controls inflammatory cytokine production by T cells and osteoclast differentiation [36] and that selective p38α inhibitors can prevent osteoclast-mediated

inflammatory osteolysis [37] and bone loss induced by estrogen deficiency [38]. However, from our observations, the long-term use of selective p38α inhibitors may cause bone tissue deterioration and therefore may not be appropriate to treat osteoclast-mediated bone loss.

**Acknowledgments** We would like to thank Sabina Troccaz and Pierre Apostolides for their expert technical assistance. We thank Professor Manolis Pasparakis for providing *p38a*$^{f/f}$ mice and Professor Thomas L. Clemens for *Ocn-Cre* mice. This work was supported by the Swiss National Science Foundation (310030-127638) and by the Novartis Foundation (Basel, Switzerland).

**Conflict of interest** The authors state that they have no conflicts of interest.

## References

1. Raggatt LJ, Partridge NC (2010) Cellular and molecular mechanisms of bone remodeling. J Biol Chem 285:25103–25108
2. Zarubin T, Han J (2005) Activation and signaling of the p38 MAP kinase pathway. Cell Res 15:11–18
3. Cuadrado A, Nebreda AR (2010) Mechanisms and functions of p38 MAPK signaling. Biochem J 429:403–417
4. Guicheux J, Lemonnier J, Ghayor C, Suzuki A, Palmer G, Caverzasio J (2003) Activation of p38 mitogen-activated protein kinase and c-Jun-NH2-terminal kinase by BMP-2 and their implication in the stimulation of osteoblastic cell differentiation. J Bone Miner Res 18:2060–2068
5. Lee KS, Hong SH, Bae SC (2002) Both the Smad and p38 MAPK pathways play a crucial role in Runx2 expression following induction by transforming growth factor-beta and bone morphogenetic protein. Oncogene 21:7156–7163
6. Suzuki A, Palmer G, Bonjour JP, Caverzasio J (1999) Regulation of alkaline phosphatase activity by p38 MAP kinase in response to activation of Gi protein-coupled receptors by epinephrine in osteoblast-like cells. Endocrinology 140:3177–3182
7. Rey A, Manen D, Rizzoli R, Ferrari SL, Caverzasio J (2007) Evidences for a role of p38 MAP kinase in the stimulation of alkaline phosphatase and matrix mineralization induced by parathyroid hormone in osteoblastic cells. Bone 41:59–67
8. Caverzasio J, Manen D (2007) Essential role of Wnt3a-mediated activation of mitogen-activated protein kinase p38 for the stimulation of alkaline phosphatase activity and matrix mineralization in C3H10T1/2 mesenchymal cells. Endocrinology 148:5323–5330
9. You J, Reilly GC, Zhen X, Yellowley CE, Chen Q, Donahue HJ, Jacobs CR (2001) Osteopontin gene regulation by oscillatory fluid flow via intracellular calcium mobilization and activation of mitogen-activated protein kinase in MC3T3-E1 osteoblasts. J Biol Chem 276:13365–13371
10. Ulsamer A, Ortuño MJ, Ruiz S, Susperregui AR, Osses N, Rosa JL, Ventura F (2008) BMP-2 induces Osterix expression through up-regulation of Dlx5 and its phosphorylation by p38. J Biol Chem 283:3816–3826
11. Ortuno MJ, Ruiz-Gaspa S, Rodriguez-Carballo E, Susperregui AR, Bartrons R, Rosa JL, Ventura F (2010) p38 regulates expression of osteoblast-specific genes by phosphorylation of Osterix. J Biol Chem 285:31985–31994
12. Greenblatt MB, Shim JH, Zou W, Sitara D, Schweitzer M, Hu D, Lotinun S, Sano Y, Baron R, Park JM, Arthur S, Xie M, Schneider MD, Zhai B, Gygi S, Davis R, Glimcher LH (2010) The p38 MAPK pathway is essential for skeletogenesis and bone homeostasis in mice. J Clin Invest 120:2457–2473
13. Zou W, Greenblatt MB, Shim JH, Kant S, Zhai B, Lotinun S, Brady N, Hu DZ, Gygi SP, Baron R, Davis RJ, Jones D, Glimcher LH (2011) MLK3 regulates bone development downstream of the faciogenital dysplasia protein FGD1 in mice. J Clin Invest 121:4383–4392
14. Whitehouse CA, Waters S, Marchbank K, Horner A, McGowan NW, Jovanovic JV, Xavier GM, Kashima TG, Cobourne MT, Richards GO, Sharpe PT, Skerry TM, Grigoriadis AE, Solomon E (2010) Neighbor of Brca1 gene (Nbr1) functions as a negative regulator of postnatal osteoblastic bone formation and p38 MAPK activity. Proc Natl Acad Sci USA 107:12913–12918
15. Heinrichsdorff J, Luedde T, Perdiguero E, Nebreda AR, Pasparakis M (2008) p38alpha MAPK inhibits JNK activation and collaborates with IkappaB kinase 2 to prevent endotoxin-induced liver failure. EMBO Rep 9:1048–1054
16. Zhang M, Xuan S, Bouxsein ML, von Stechow D, Akeno N, Faugere MC, Malluche H, Zhao G, Rosen CJ, Efstratiadis A, Clemens TL (2002) Osteoblast-specific knockout of the insulin-like growth factor (IGF) receptor gene reveals an essential role of IGF signaling in bone matrix mineralization. J Biol Chem 277:44005–44012
17. Adams RH, Porras A, Alonso G, Jones M, Vintersten K, Panelli S, Valladares A, Perez L, Klein R, Nebreda AR (2000) Essential role of p38alpha MAP kinase in placental but not embryonic cardiovascular development. Mol Cell 6:109–116
18. Bonnet N, Standley KN, Bianchi EN, Stadelmann V, Foti M, Conway SJ, Ferrari SL (2009) The matricellular protein periostin is required for SOST inhibition and the anabolic response to mechanical loading and physical activity. J Biol Chem 284:35939–35950
19. Zhu H, Guo ZK, Jiang XX, Li H, Wang XY, Yao HY, Zhang Y, Mao N (2010) A protocol for isolation and culture of mesenchymal stem cells from mouse compact bone. Nat Protoc 5:550–560
20. Canalis E (2010) Update in new anabolic therapies for osteoporosis. J Clin Endocrinol Metab 95:1496–1504
21. Trivedi R, Goswami R, Chattopadhyay N (2010) Investigational anabolic therapies for osteoporosis. Expert Opin Investig Drugs 19:995–1005
22. Marie PJ, Kassem M (2011) Osteoblasts in osteoporosis: past, emerging, and future anabolic targets. Eur J Endocrinol 165:1–10
23. Ducy P, Starbuck M, Priemel M, Shen J, Pinero G, Geoffroy V, Amling M, Karsenty G (1999) A Cbfa1-dependent genetic pathway controls bone formation beyond embryonic development. Genes Dev 13:1025–1036
24. Baek WY, Lee MA, Jung JW, Kim SY, Akiyama H, de Crombrugghe B, Kim JE (2009) Positive regulation of adult bone formation by osteoblast-specific transcription factor osterix. J Bone Miner Res 24:1055–1065
25. Yang X, Matsuda K, Bialek P, Jacquot S, Masuoka HC, Schinke T, Li L, Brancorsini S, Sassone-Corsi P, Townes TM, Hanauer A, Karsenty G (2004) ATF4 is a substrate of RSK2 and an essential regulator of osteoblast biology; implication for Coffin-Lowry Syndrome. Cell 117:387–398
26. Mak KK, Bi Y, Wan C, Chuang PT, Clemens T, Young M, Yang Y (2008) Hedgehog signaling in mature osteoblasts regulates bone formation and resorption by controlling PTHrP and RANKL expression. Dev Cell 14:674–688
27. Baron R, Rawadi G, Roman–Roman S (2006) Wnt signaling: a key regulator of bone mass. Curr Top Dev Biol 76:103–127
28. Zhao M, Harris SE, Horn D, Geng Z, Nishimura R, Mundy GR, Chen D (2002) Bone morphogenetic protein receptor signaling is necessary for normal murine postnatal bone formation. J Cell Biol 157:1049–1060

29. Yoshida Y, Tanaka S, Umemori H, Minowa O, Usui M, Ikematsu N, Hosoda E, Imamura T, Kuno J, Yamashita T, Miyazono K, Noda M, Noda T, Yamamoto T (2000) Negative regulation of BMP/Smad signaling by Tob in osteoblasts. Cell 103:1085–1097
30. Tan X, Weng T, Zhang J, Wang J, Li W, Wan H, Lan Y, Cheng X, Hou N, Liu H, Ding J, Lin F, Yang R, Gao X, Chen D, Yang X (2007) Smad4 is required for maintaining normal murine postnatal bone homeostasis. J Cell Sci 120:2162–2170
31. Yamashita M, Ying SX, Zhang GM, Li C, Cheng SY, Deng CX, Zhang YE (2005) Ubiquitin ligase Smurf1 controls osteoblast activity and bone homeostasis by targeting MEKK2 for degradation. Cell 121:101–113
32. Takeda S, Elefteriou F, Levasseur R, Liu X, Zhao L, Parker KL, Armstrong D, Ducy P, Karsenty G (2002) Leptin regulates bone formation via the sympathetic nervous system. Cell 111:305–317
33. Fulzele K, Riddle RC, DiGirolamo DJ, Cao X, Wan C, Chen D, Faugere MC, Aja S, Hussain MA, Brüning JC, Clemens TL (2010) Insulin receptor signaling in osteoblasts regulates postnatal bone acquisition and body composition. Cell 142:309–319
34. Amizuka N, Karaplis AC, Henderson JE, Warshawsky H, Lipman ML, Matsuki Y, Ejiri S, Tanaka M, Izumi N, Ozawa H, Goltzman D (1996) Haploinsufficiency of parathyroid hormone-related peptide (PTHrP) results in abnormal postnatal bone development. Dev Biol 175:166–176
35. Richman C, Kutilek S, Miyakoshi N, Srivastava AK, Beamer WG, Donahue LR, Rosen CJ, Wergedal JE, Baylink DJ, Mohan S (2001) Postnatal and pubertal skeletal changes contribute predominantly to the differences in peak bone density between C3H/HeJ and C57BL/6J mice. J Bone Miner Res 16:386–397
36. Schieven GL (2009) The p38alpha kinase plays a central role in inflammation. Curr Top Med Chem 9:1038–1048
37. Mbalaviele G, Anderson G, Jones A, De Ciechi P, Settle S, Mnich S, Thiede M, Abu-Amer Y, Portanova J, Monahan J (2006) Inhibition of p38 mitogen-activated protein kinase prevents inflammatory bone destruction. J Pharmacol Exp Ther 317:1044–1053
38. Caverzasio J, Higgins L, Ammann P (2008) Prevention of trabecular bone loss induced by estrogen deficiency by a selective p38alpha inhibitor. J Bone Miner Res 23:1389–1397